Ion track formation in amorphous SiO_2: a low velocity study

M. Karlušić[1*], M. Škrabić[2], M. Majer[1], M. Buljan[1], V. Skuratov[3,4,5], H.K. Jung[6], O.Gamulin[2], M. Jakšić[1]

1 Ruđer Bošković Institute, Bijenička cesta 54, 10000 Zagreb, Croatia
2 University of Zagreb, School of Medicine, Šalata 3, 10000 Zagreb, Croatia
3 Joint Institute for Nuclear Research, Dubna, Russia
4 National Research Nuclear University MEPhI, Moscow, Russia
5 Dubna State University, Dubna, Russia
6 Korea Atomic Energy Research Institute, Daejeon, Republic of Korea
** corresponding author: marko.karlusic@irb.hr*

Abstract

Ion track formation in amorphous SiO_2 was investigated using infrared spectroscopy. For comparison, one set of samples was also irradiated using 1.25 MeV gamma rays. Increase of 1044 cm^{-1} peak and decrease of 1078 cm^{-1} peak was observed in all cases. Experimental results were analyzed using analytical thermal spike model and non-standard model parameters were found. This finding is attributed to the amorphous structure of the a-SiO_2 material.

Keywords: swift heavy ion, ion track, thermal spike, amorphous SiO_2, infrared spectroscopy, gamma rays

1. Introduction

Permanent damage formed after the passage of a swift heavy ion (SHI) through a solid material is called the ion track [1–6]. Most common description of the ion track formation, the thermal spike model, proposes that the kinetic energy of the projectile, deposited as dense electronic excitation along the ion trajectory, can lead to melting of the material. In this case, ion tracks originate from the quenching of the molten phase on the nanosecond time scale, resulting in an amorphous inclusion. In crystal materials, ion tracks can be readily observed with various techniques like electron microscopy or Rutherford backscattering spectrometry in channeling [5,7,8]. Atomic force microscopy has also been found suitable for direct imaging of ion tracks on the surface after grazing SHI irradiations [9–16]. However, in amorphous materials, investigation of ion tracks is much more difficult due to the weak contrast between the ion track and the surrounding material, hence very few techniques like infrared (IR) spectroscopy and small angle X-ray scattering (SAXS) were found

suitable for this purpose [17–19].

Response of the amorphous SiO_2 (a-SiO_2, vitreous silica) to SHI irradiation has been thoroughly studied in the past because of the material's importance for industrial applications in electronics and photonics. Furthermore, a-SiO_2 is a role model for glass structures and therefore important for studies where similar materials are exposed to fission fragment damage during nuclear waste immobilisation [20]. Optical fibers based on a-SiO_2 can also be used for the distributed measurements of high temperatures and high radiation levels at various nuclear facilities [21,22]. Unlike crystalline materials that can undergo large structural changes due to exposure to high levels of radiation [23,24], amorphous materials should not alter much since their structure remains amorphous [25]. Therefore, ion track formation in a-SiO_2 due to SHI irradiation has been studied for many years now [17,18,26–33] and recently a review has been published [20]. Other SHI irradiation effects in a-SiO_2 have also been researched thoroughly, most notably plastic deformation (ion hammering effect) [34–38] and nanoparticles modification/synthesis [19,39–49], but also ion track etching [50–52], surface nanostructuring [11,53–55] and sputtering [56–60].

Often are these experimental results described using thermal spike models [18,20,32,35,61–66] which can quantitatively explain various observed features. Some difficulties, for example the role of self-trapped excitons, remained unclear in the ion track formation processes [3,6,64,65,67,68]. Also, theoretical efforts indicated that a significant amount of SHI deposited energy remains stored in the valence holes within the ion tracks in a-SiO_2 and is released only on the picosecond time-scale via Auger processes [69–72]. Experimental and theoretical efforts investigating these early stages of ion track formation via detection of SHI induced X-rays and secondary electrons are still ongoing [73–77]. It might be that these features of ion track formation in a-SiO_2 led some authors to apply diverse, non-standard parameters in thermal spike calculations [19,48,65,78].

Aim of this work is to obtain new experimental data from which thermal spike parameters for a-SiO_2 can be established. To accomplish this, we have performed low velocity SHI irradiations (E/A < 2 MeV/amu) of the samples and analysed them using IR spectroscopy. Additionally, we have performed high dose gamma ray (GR) irradiations and characterised the samples with the same method. This way, correlation in radiation effects between SHI and GR irradiation was established. In this work we follow well-established approach of using IR spectroscopy to characterise ion tracks in a-SiO_2 [17,18,26–28,32]. Evolution of the TO3 band seen as a decrease of 1078 cm^{-1} peak and increase of 1044 cm^{-1} peak has been observed with increasing SHI fluence. These changes have been

attributed to the decrease of the O-Si-O bond angle from 144° to 129° due to compaction of silica [28]. Microscopically, origin of this structural damage has been found in the change of a-SiO_2 from large (six member) ring structure to small (planar three and four member) ring structure [18,28,29]. It has also been experimentally observed that the absorption band attributed to LO4-TO4 pair at 1165-1200 cm^{-1} does not change upon irradiation [18]. Ion track sizes evaluated from observed kinetics have been found in a very good agreement with SAXS data [17,18] and consistent with track etching results [52]. This enables comprehensive analysis of the ion track data in a-SiO_2 both from previous and present study.

2. Experimental details

Thermally grown a-SiO_2 film on Si wafer and having 200 nm thickness was purchased from Crystec (Berlin, Germany). Oxide was grown on both sides of the Si wafer that was cut into roughly 1x1 cm^2 pieces before irradiation. No further sample preparation was done.

First set of samples was irradiated at normal incidence using 1 MeV O, 3 MeV O and 23 MeV I delivered by 6 MV EN Tandem Van de Graaff accelerator at the Ruđer Bošković Institute (RBI, Zagreb, Croatia). Second set of samples was irradiated at 30° off normal using 167 MeV Xe beams delivered by cyclotron at Joint institute for Nuclear Research (JINR, Dubna, Russia). Fluences applied were up to 3×10^{15} ions/cm^2 for oxygen beams, up to the 3×10^{13} ions/cm^2 for the iodine beam, and up to the 10^{13} ions/cm^2 for the xenon beam. Third set of samples was exposed to 1.25 MeV GR irradiation up to a dose of 90 MGy using panoramic ^{60}Co source at the RBI.

For the sample analysis, IR spectroscopy was performed using PerkinElmer Spectrum GX spectrometer equipped with DTGS (Deuterated TriGlycine Sulfate) detector. FTIR spectra were recorded in normal transmission mode averaging 20 scans over the range 400-2000 cm^{-1}. Before scanning the samples the background was recorded collecting 50 scans with a spectral resolution of 4 cm^{-1}.

3. Results

For a given SHI beam, samples were irradiated with different fluences and following this IR spectra were measured. The spectra were subsequently baseline corrected. As an example, IR spectrum

from the sample irradiated by 23 MeV I beam is shown on Fig. 1a. From the analysis of the recorded spectra, it is clearly seen how 1078 cm^{-1} peak decreases with ion fluence, while 1044 cm^{-1} peak increases, as shown on Figs. 1b.-1e for different ion beams. There is no significant change in the intensity of the pair LO4-TO4 band at 1165-1200 cm^{-1}. It can also be seen that 1078 cm^{-1} peak does not dissapear because there is a contribution from the unirradiated a-SiO_2 film on the backside of the Si wafer. In contrast to the previous work [18], we find somewhat different film thickness on the backside because the Si wafer has been polished only on the side facing ion beam.

Since the positions of band maxima are well known [20], Gaussian fitting of the nonirradiated sample with fixed peak positions (wavenumbers 1044, 1078, 1185 cm^{-1}) was performed and virgin band areas were obtained. The same fitting procedure was repeated for all irradiated samples. Our fitting procedure is different from the ones in refs. [18, 32] where fitting was done with fixed full widths at half maximum (FWHM) of each band. Most of the oscillators in virgin SiO_2 samples vibrate with frequency of 1078 cm^{-1} (144° bond angle) and there are, if any, only small number of oscillators with rather narrow energy distribution which vibrate with frequency of 1044 cm^{-1} (129° bond angle). As seen from experiments, irradiation of the samples influences structural reordering of the molecules, attributed to the change of the O-Si-O bond angle, in which the number of oscillators with smaller bond angle increases. Apart from the change of the number of oscillators, it is to be expected that irradiation causes certain system disorder which would manifest as broader vibrational energy dispersion of the oscillators i.e. width of the 1044 cm^{-1} band. On the other hand, positions of the band maxima, which correspond to the mean frequencies of the vibrational bands, are not changed with irradiation. Therefore, it is to be expected that Gaussian fitting with fixed positions of the band maxima would yield more accurate description of the physical situation. Indeed, we have found that our spectra showed better fits with fixed positions of each peak. In our fitting procedure, FWHMs of the 1078 cm^{-1} and 1185 cm^{-1} band in all samples vary approximately 5% (at most 10%), what can be attributed to the fluence uncertainties, while the FWHM of the 1044 cm^{-1} band increases with fluence until saturation is reached. All this is in accordance with ref. [79] where it is shown that the width of the TO band is proportional to the mean square deviation of the bond angle in amorphous materials.

Gaussian peak areas obtained using above methodology exhibit uniform evolution with respect to the applied SHI fluence as shown on Fig. 1. To deduce ion track cross-section $B=r^2\pi$, the Poisson law is used for fitting evolution of 1078 cm^{-1} peak area Z and 1044 cm^{-1} peak area Y with increasing SHI fluence F:

$$Z(F) = [Z_0(F=0) - Z_{min}(F=\infty)] \times e^{-B \times F} + Z_{min}(F=\infty) \quad \text{(eq 1)}$$

$$Y(F) = [Y_{max}(F=\infty) - Y_0(F=0)] \times (1 - e^{-B \times F}) + Y_0(F=0) \quad \text{(eq 2)}$$

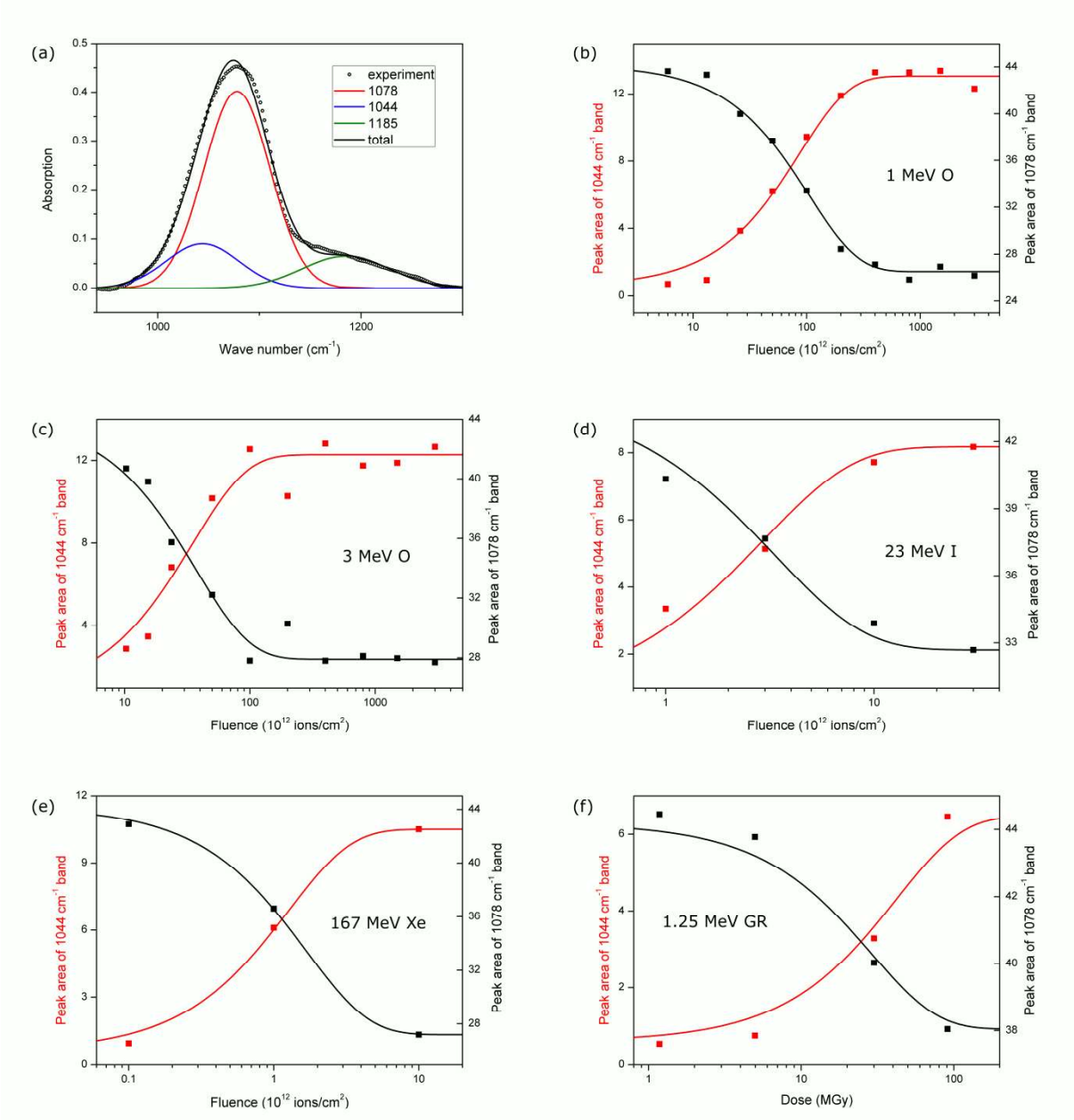

Figure 1. (a) IR absorption spectrum from irradiated a-SiO_2 in the range of the TO3 band. Measured IR spectrum (23 MeV I, fluence $3x10^{13}$ ions/cm^2) is fitted using three Gaussians with peaks centered at 1044 cm^{-1}, 1078 cm^{-1}, and 1185 cm^{-1}. Evolution of the TO3 band with increasing fluence for (b) 1 MeV O, (c) 3 MeV O, (d) 23 MeV I, and (e) 167 MeV Xe beam. (f) Evolution of the TO3 band with increasing dose for 1.25 MeV GR irradiation.

For the measured ion track cross sections, their average values determined from IR spectroscopy of 1078 cm^{-1} and 1044 cm^{-1} peaks are plotted, and all evaluated cross sections are reported in Table 1. Error bars represent dispersion of the 1078 cm^{-1} and 1044 cm^{-1} peak data [18]. In the case of non-normal irradiation geometry for the Xe beam, damage cross section was corrected by the geometrical factor. Finally, on Fig. 1f. we present spectra from the GR irradiated samples. Changes in the TO3 band of the IR spectra are visible only for the two highest doses, and show similar behaviour to the SHI irradiated samples. It should be noted that in this case both front side and backside of the a-SiO_2 film are affected by the GR irradiation.

Ion beam	Electronic stopping (keV/nm)	Nuclear stopping (keV/nm)	Range (μm)	Damage cross section σ_{1078} (nm^2)	Damage cross section σ_{1044} (nm^2)	Average damage cross section σ (nm^2)
1 MeV O	0.974	0.019	1.66	0.96 ± 0.05	1.15 ± 0.09	1.06 ± 0.1
3 MeV O	1.679	0.008	3.09	2.68 ± 0.26	2.86 ± 0.38	2.77 ± 0.09
23 MeV I	5.214	0.257	7.19	29.9 ± 3.7	34.1 ± 3.9	32 ± 2.1
167 MeV Xe	13.91	0.058	19.43	51.7 ± 2.1	68.6 ± 5.6	60.15 ± 8.45

Table 1. Damage cross sections σ measured by IR spectroscopy for the TO3 band (1078 cm^{-1} and 1044 cm^{-1} peaks). SHI irradiation parameters calculated using SRIM [80] for a-SiO_2 with density 2.2 g/cm^3.

4. Discussion

Despite many similarities, two of the most commonly used thermal spike models, namely inelastic thermal spike model (ITSM) and analytical thermal spike model (ATSM), are at present mutually incompatible [81]. It is no surprise that experimental evidence for either validation or refutation of both models is vigorously sought-after via ion-track experiments [5,7,82–85]. Also other SHI irradiation effects were considered with the same purpose, like sputtering [60,86,87], ion hammering [61,65], ion beam mixing [88–90] and nanohillock formation [14,91–95]. Since the present work aims to investigate applicability of ATSM for description of ion tracks in a-SiO_2, here we summarize model equations [83]:

$$R^2 = a_0^2 \ln \frac{S_e}{S_{et}} \qquad S_{et} < S_e < eS_{et} \qquad \text{(eq 3)}$$

$$R^2 = \frac{a_0^2}{e}\frac{S_e}{S_{et}} \qquad eS_{et} < S_e \qquad \text{(eq 4)}$$

$$S_{et} = \frac{\rho c \Delta T_m a_0^2 \pi}{g} \qquad \text{(eq 5)}$$

For crystalline insulators, ATSM parameters have been established as a_0 = 4.5 nm and g = 0.4 or g = 0.17, for low (E/A < 2 MeV/A) and high (E/A > 8 MeV/A) velocity irradiations, respectively. For the intermediate velocities (2 MeV/A < E/A < 8 MeV/A) parameter g can have intermediate value. These model parameters have been questioned in the case of quartz [5], but later experimental work seems to reaffirm canonical ATSM interpretation [23] as well as previous observation of unusual dispersion of the old experimental data [96]. In the case of a-SiO_2, non-standard model parameters have been used previously, when increase in factor g = 0.6 has been seen [65], or alternatively decrease of the a_0 = 3.5 nm [19,48] or even to a_0 = 2.8 nm [78] has been proposed. Furthermore, the velocity effect has been observed at lower ion velocities [7,48], and very recently it was reported that parameter g can be dependent on the electronic stopping power [97]. Given all these developments, and taking into account that a-SiO_2 is more susceptible to ion track formation due to stronger electron-phonon coupling [98] and lower melting temperature [99], it is of importance to reliably establish ATSM parameters needed to succesfully describe ion tracks in amorphous SiO_2. Procedure to establish ATSM parameteres is the following [83]: from the logarithmic regime (i.e. data described by (Eq. 3)) parameter a_0 can be extracted by applying the least squares fit on the data in the semilogarithmic graph, when the slope of the fitted line equals a_0^2. Also, from the same fit, the threshold S_{et} can be determined. Next, by substituting (Eq. 5) into (Eq. 4), one can use least squares method from data in the linear regime (i.e. data described by (Eq.4)) to determine ATSM parameter g. Ideally, this value should be consistent with the value of g that could be numerically calculated from (Eq. 5). In principle, the same procedure could be applied to high velocity data points, but usually very high stopping powers are needed to have sufficient amount of experimental data for thorough analysis.

4.1. Establishing ATSM parameters for a-SiO_2

Ion tracks in both quartz SiO_2 [23,100,101] and a-SiO_2 have shown some peculiarities that turned out to be important for thermal spike models. In the 1990s, when the amount of experimental data was not yet large, ion tracks in quartz SiO_2 and a-SiO_2 appeared of the same size [26,61,100], and respective thresholds for ion track formation have been found to be very close. Not surprisingly, thermal spike models initially used the same parameters for both quartz and a-SiO_2 [61,88]. In case of ITSM, the difference between these two materials (i.e. greater a-SiO_2 sensitivity to SHI irradiation)

has been noticed earlier and relevant model parameter, electron-phonon mean free path, has been evaluated as λ = 4 nm for quartz SiO_2 and λ = 2.5 nm for a-SiO_2 [63]. These values have been fine tuned over the years and recently λ = 3.6 nm for quartz SiO_2 [86] and both λ = 2.5 nm and λ = 3 nm for a-SiO_2 have been reported [18,60]. Later it was recognized that standard ATSM parameters for crystalline insulators [83] are also not suitable for description of ion tracks in a-SiO_2 [19,48,65,78].

To establish ATSM parameters for a-SiO_2, we now analyse both here presented new experimental data on ion tracks in a-SiO_2, as well as previously published data using the same methodology (IR spectroscopy) [17,18,26–28,32]. For comparison, we also analyse recent results from optical reflectivity (OR) measurements [102]. First, we restrict our analysis only to data where contribution of the nuclear stopping can be neglected i.e. where ratio between the two is at least one order of magnitude. In the analysis, also included are experimental data from the transmission electron microscopy (TEM) and small angle X-ray scattering (SAXS) because total size of the core-shell track observed by SAXS is in agreement with the results of the IR measurements [18]. We list published and here measured experimental data in Table 2.

Ion	Energy (MeV)	Energy per nucleon (MeV/A)	Electronic stopping (keV/nm)	Nuclear stopping (keV/nm)	Ion track cross section (nm^2)	Technique and Reference
Xe	762	5.77	15.7	0.02	80	IR, [26]
Ni	551	9.5	4.99	0.003	6	IR, [26]
Au	22. 5	0.11	3.84	0.7	18.1 ± 3.0	SAXS, [17]
Au	45.7	0.23	7.32	0.43	55.4 ± 2.6	SAXS, [17]
Au	77.2	0.39	10.97	0.29	75.4 ± 3.1	SAXS, [17]
Au	168.3	0.85	16.17	0.16	91.6 ± 3.4	SAXS, [17]
Xe	628	4.76	16.02	0.02	58.1 ± 5.4	SAXS, [17]
Xe	1416	10.73	13.67	0.01	50.3 ± 7.5	SAXS, [17]
O	3.1	0.19	1.69	0.007	3.8 ± 0.7	IR, [18]
Si	5.5	0.2	2.77	0.02	14 ± 4	IR, [18]
Ni	11.4	0.2	3.89	0.08	27 ± 6	IR, [18]
O	3.1	0.19	1.69	0.007	3.8 ± 1.4	TEM, [18]
Si	5.5	0.2	2.77	0.02	13.9 ± 4	TEM, [18]
Ni	11.4	0.2	3.89	0.08	26.4 ± 9.1	TEM, [18]
C	66	5.5	0.47	0.0003	0	IR, [32]

S	160	5	2.69	0.002	2.8 ± 0.5	IR, [32]
Ni	320	5	6.22	0.005	16 ± 2	IR, [32]
Sn	616	5.5	14.48	0.015	69 ± 9	IR, [32]
Xe	645	5	16	0.018	62 ± 9	IR, [32]
Pb	957	4.6	22.95	0.042	151 ± 25	IR, [32]
F	5	0.26	2.09	0.004	3.5	OR, [102]
Br	5	0.06	2.08	0.265	9.7	OR, [102]
Br	10	0.13	3.48	0.16	13.5	OR, [102]
Br	15	0.19	4.48	0.119	22.2	OR, [102]
Br	25	0.32	5.76	0.08	38.7	OR, [102]
Br	40	0.51	6.92	0.055	44.7	OR, [102]
O	0.9	0.06	0.91	0.02	1.06 ± 0.1	IR, here
O	2.92	0.18	1.67	0.008	2.77 ± 0.09	IR, here
I	22.5	0.18	5.13	0.261	32 ± 2.1	IR, here
Xe	166	1.26	13.89	0.058	60.15 ± 8.45	IR, here

Table 2. Measured ion track radii and related cross sections in a-SiO_2 using IR, SAXS, TEM and OR, either previously published with corresponding reference, or measured in this work. The SHI kinetic energy is calculated at the mid-point of thin a-SiO_2 film. All stopping powers are calculated using SRIM 2013 code [80].

As shown on Fig. 2a, velocity effect is active already at 1 MeV/A, in agreement with our previous work [48]. Thus, for the analysis of the low velocity data points we consider only data acquired from irradiations with specific kinetic energies below E/A = 0.5 MeV/A. Experimental data from irradiations with specific kinetic energy above 0.85 MeV/A are treated as high-velocity data points.

First, we consider low-velocity data points. The threshold for the ion track formation S_{et} = 1.50 ± 0.25 keV/nm is found analysing the data from the logarithmic regime (Eq. 3) occurring below 4 keV/nm in electronic stopping power. From the same data subset, ATSM parameter a_0 = 2.7 ± 0.2 nm is found, in agreement with previous work [78]. Analysing the data from the linear regime, ATSM parameter g = 0.53 ± 0.02 was established by fitting the experimental data to (Eq. 4). By taking into account established ion track formation threshold of S_{et} = 1.50 ± 0.25 keV/nm, the analysis yields a_0 = 3.4 ± 0.3 nm for data points from linear regime. This way we conclude the ATSM parameters for low velocity irradiations are a_0 = 3.0 ± 0.5 nm and g = 0.53 ± 0.02. Using these values (Eq. 4),

calculated threshold for ion track formation S_{et} = 1.53 ± 0.28 keV/nm, in excellent agreement with experimentally determined value.

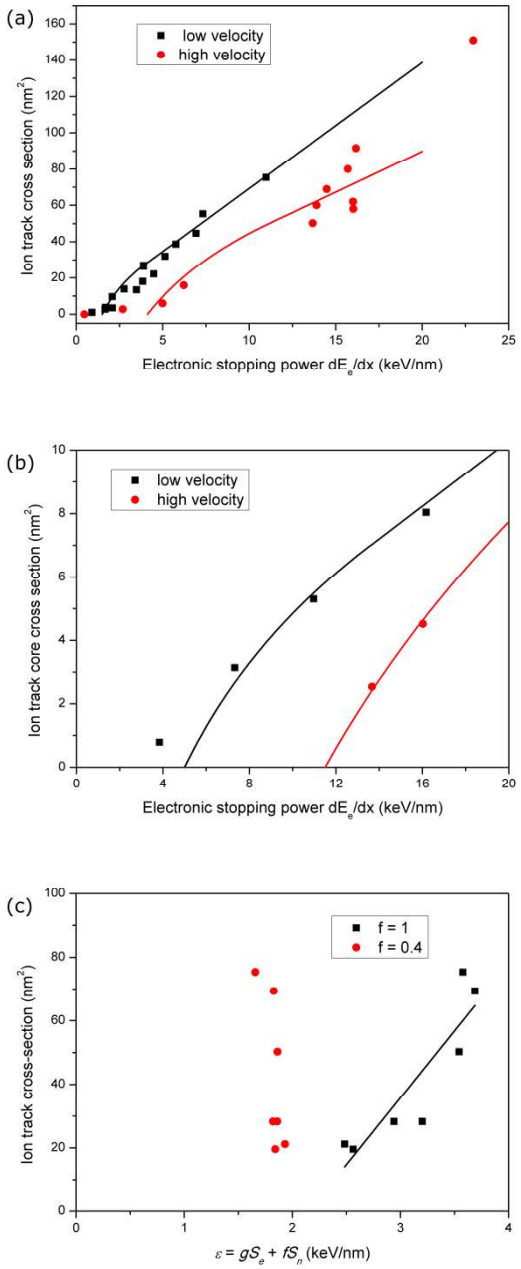

Figure 2. (a) Ion tracks in a-SiO_2 after low velocity irradiations (black) and high velocity irradiations (red). The ATSM model predictions are plotted for comparison. (b) Ion tracks cores in a-SiO_2 after low velocity irradiations (black) and high velocity irradiations (red). The ATSM model predictions are plotted for comparison. (c) Damage cross section dependence on the density of deposited energy for two different scenarios: very efficient energy transfer of nuclear stopping (f=1) and standard transfer rate of electronic stopping (f=0.4). The ATSM model prediction is plotted for comparison.

As often is the case, very small ion tracks can be found below the threshold established by the least squares method, which are usually neglected in the analysis [83]. In our case, this is 1 MeV O data point, which we do not include into the present analysis. However, as can be seen from comparing Figs. 1b and 1c, differences between 1 MeV O and 3 MeV O are not that large and could point to other track forming mechanism below the threshold established by the thermal spike model, like for example excitonic mechanism [3]. Present work can open up the way for future studies of near threshold ion track damage formation, that should shed light on this open question [23]. Generalization of the analysis to Avrami-type behaviour [103,104] could be well justified for these irradiation conditions.

Next, we consider the high-velocity data subset. There are only two data points above 8 MeV/A, but as can be seen on Fig.2a, 0.85 MeV/A gold and 1.26 MeV/A xenon irradiations can be included into this data set, as well as a number of irradiations with ion velocities of 5 MeV/A. Below-threshold datapoint of 5 MeV/A carbon ion beam is neglecetd. Still, two data points can be found in the logarithmic regime (Eq. 4), indicating larger value of the ATSM parameter a_0 = 4 nm for high velocity irradiations. Using the same procedure as before, we analysed the linear regime between 10-20 keV/nm to obtain ATSM parameter g = 0.35 ± 0.02 for the high velocity irradiations. Data point from 5 MeV/A lead ion irradiation was not used in the analysis because as an outlier it was not possible to incorporate it in the present analysis. Taking into account changes to ATSM parameters, the high velocity threshold for ion track formation is estimated at S_{et} = 4.1 keV/nm.

As shown in Fig. 2a, plotted curves using ATSM parameters (a_0 = 3 nm, g = 0.53) for low velocity and (a_0 = 4 nm, g = 0.35) for high velocity irradiations follow experimental data well. Velocity effect is clearly observed, but separation between high and low velocity data occurs already at 1 MeV/A, similar to the case of CaF_2 [7] and Ge containing a-SiO_2 [48]. Although it is difficult to maintain assignment of the standard ATSM values g = 0.17 to pure thermal spike and g = 0.4 to Coulomb explosion contribution, we note high velocity ATSM parameters have values close to the standard ATSM parameters for the low velocity irradiation. This would implicate that Coulomb explosion is active even for irradiations using the highest ion velocities at 10 MeV/A, but more experimental data is needed to verify this.

However, the most puzzling values of the ATSM parameters are for the low velocity irradiations. These non-standard values are needed to correctly describe low threshold for ion track formation, as well as ion track sizes in this regime. As proposed before, possible explanation can be related to the amorphous structure of the a-SiO_2 material. The velocity effect, as it is conceived in

the ITSM, i.e. high density of deposited energy after low velocity irradiations as a consequence of limited spread of excited electrons in the primary stages of the ion track formation, could possibly be promoted even further by amorphous structure of the material and its low thermal conductivity. Thus, very narrow cylinder (a_0 < 4.5 nm) of highly excited (g > 0.4) matter along ion trajectory, as suggested by ATSM parameters, could be responsible for observed ion track features. Similar conclusion has very recently been reached by molecular dynamics studies of ion track formation in a-SiO_2 [102].

4.2. Extending ATSM to description of ion track core and additive role of nuclear stopping in a-SiO_2

Two features of ion tracks in a-SiO_2 have been used previously to support validity of the ITSM description of ion tracks in this material: appearance of the underdense ion track core for very high electronic stopping powers [17], and additivity of the electronic and nuclear stopping power as source term in the ITSM equations [18]. The observation of the underdense core in SAXS measurements have been assigned to very high densities of deposited energy leading to increase of the material temperature above the boiling point of 7000 K [17]. Results of the molecular dynamics simulations agree well with experimental data [17,102]. In the Table 3 we list available experimental data on measured radii of the ion track cores in a-SiO_2 [17].

Ion	Energy (MeV)	Energy per nucleon (MeV/A)	Electronic stopping (keV/nm)	Nuclear stopping (keV/nm)	Ion track core cross section (nm^2)	Technique and Reference
Au	22. 5	0.11	3.84	0.7	0.79 ± 0.47	SAXS, [17]
Au	45.7	0.23	7.32	0.43	3.14 ± 0.94	SAXS, [17]
Au	77.2	0.39	10.97	0.29	5.31 ± 0.82	SAXS, [17]
Au	168.3	0.85	16.17	0.16	8.04 ± 1.01	SAXS, [17]
Xe	628	4.76	16.02	0.02	4.52 ± 1.51	SAXS, [17]
Xe	1416	10.73	13.67	0.01	2.54 ± 1.13	SAXS, [17]

Table 3. Measured ion track core radii and calculated core cross sections in a-SiO_2 using SAXS [17]

Due to scarcity of data, we do not perform the analysis in the manner described in the section 4.1. Instead, as shown on Fig. 2b, we plot available experimental data together with estimated ATSM parameters that ensure satisfactory fit. We estimate initial widths of the thermal spike as a_0 = 1.5 nm for low velocity irradiations, and a_0 = 2.1 nm for high velocity irradiations. These

values are much smaller than ATSM parameter a_0 deduced from ion track radii measurements in section 4.1., but decrease of a_0 with increase in the deposited energy density is consistent with results from section 4.1., indicating highly localized ultrafast processes on the nanoscale. Furthermore, by estimating thresholds for appearance of the underdense ion track core at 5 keV/nm for low velocity and at 11.5 keV/nm for high velocity irradiations, by means of (eq. 5), other ATSM parameter g can be evaluated. By imposing material boiling at 7000 K as requirement for appearance of the underdense ion track core, g = 0.16 for low velocity irradiations, and g = 0.135 for high velocity irradiations can be found. These values are very close to standard ATSM parameter g = 0.17 for high velocity irradiations, assigned to pure thermal spike process. Alternatively, by imposing material melting as requirement for appearance of the underdense ion track core, g = 0.64 for low velocity irradiations, and g = 0.54 for high velocity irradiations can be found, indicating Coulomb explosion mechanism, and in very good agreement with values obtained in section 4.1. At present it is not possible to rule out any of these two possibilities, because from (Eq. 5) only ratio between temperature increase and ATSM parameter g can be found. Boiling of the material as ITSM requirement for small ion track sizes in CaF_2 has been criticized previously [7,105], and this criticism can be extended to track cores in a-SiO_2 as well. ATSM opens up another route for ion track core formation, related to melting of the material, thus avoiding the controvesy, but clearly more experimental data is needed to verify this hypothesis.

Next, we look into remaining experimental data published in ref. [18] where ion tracks were produced using Au ion beams having energies between 0.5 MeV and 15 MeV. In this energy range, electronic and nuclear stopping have comparable values. Good agreement between ITSM and experimental data has been achieved when nuclear stopping power has also been included as a source term of excitation in differential equation describing evolution of the temperature of the atomic subsystem. The agreement has been improved when stopping power values calculated by the SRIM have been determined applying reciprocity principle of Sigmund [106]. The same data is used here in order to extract ATSM parameters describing nuclear stopping contribution to the ion track formation, using the same approach that has been used previously by Szenes to describe ion tracks on muscovite mica surface [91]. In that work, increase of the ATSM parameter g up to 0.9 has been found, indicating very efficient energy transfer in case of nuclear stopping. Similar efficient transfer of deposited energy (via nuclear stopping) has been found in the case of amorphous Al_2O_3 [78].

Ion	Energy (MeV)	Energy per nucleon (MeV/A)	Electronic stopping (keV/nm)	Nuclear stopping (keV/nm)	Ion track cross section (nm^2)	Technique and Reference
Au	0.3	0.0015	0.71	3.2	75.4 ± 24.6	IR [18]
Au	0.6	0.003	1.11	3.1	69.4 ± 20.7	IR [18]
Au	1.3	0.0066	1.4	2.8	50.3 ± 15.1	IR [18]
Au	2.3	0.012	1.7	2.3	28.3 ± 9.4	IR [18]
Au	4.8	0.024	2.15	1.8	28.3 ± 9.4	IR [18]
Au	9.8	0.05	2.57	1.2	19.6 ± 6.3	IR [18]
Au	14.8	0.075	2.95	0.92	21.2 ± 6.5	IR [18]

Table 4. Measured ion track radii and calculated ion track cross sections in a-SiO_2 using IR spectroscopy measurements [18]. Electronic stopping power is tabulated from ref. [18] where reciprocity principle has been used.

As shown in Fig. 2c, considering electronic and nuclear stopping on equal footing is not realistic within ATSM framework. Only for very efficient transfer of the deposited energy from nuclear stopping into the thermal spike, reasonable behaviour can be achieved. The threshold for damage formation at 2 keV/nm is in reasonable agreement with the threshold for ion track formation found at 1.5 keV/nm. Still, ATSM parameters needed to describe observed damage behaviour originating from nuclear stopping are very much different than parameters found in section 4.1. Besides f = 1 that is in agreement with previous works on nuclear stopping contribution to the thermal spike [78,91], another ATSM parameter should be close to the standard value for insulators a_0 = 4.5 nm. At present, these ATSM parameters are given only as estimates because most of the data is clustered between 2.5 - 3.5 keV/nm. To establish their values reliably, more experimental data is needed in wider range of stopping powers.

4.3. Gamma rays and swift heavy ions: a comparison

The original idea underlying this study was to investigate if GR irradiation effects in a-SiO_2 could be imitated by SHI irradiation. This would open up a way to simulate radiation response of the material to high dose GR irradiation using SHI irradiation, which should be doable on much shorter time-scale. For example, in this study we have exposed a-SiO_2 samples to a very high dose GR irradiation in multi-month exposures, while even highest fluences of SHI irradiation were accomplished in a

matter of hours. Clearly, ion track formation is a unique feature of SHI irradiation, so we turned to SHI irradiation under conditions when electronic stopping power was under threshold for ion track formation. This way we ensured that atomic rearrangements would occur after similar electronic excitation, but no large-scale defects (i.e. ion track formation) would take place. To accomplish this, we have applied 1 MeV O (below threshold) and 3 MeV O (at the ion track formation threshold) irradiations and compared the results with the IR spectra from GR irradiated samples.

As shown on Fig. 1f, significant changes to the TO3 band in the IR spectra of GR irradiated samples occur only for highest doses of 30 MGy and 90 MGy. The GR irradiations with doses up to 10 MGy do not produce significant changes. Comparing with the 1 MeV O irradiated samples, we observe similar IR spectra changes in the range of ion fluences between 3×10^{13} – 3×10^{14} ions/cm^2. We note that required GR doses and SHI fluences agree very well with the criterion used in the work by Awazu et al. [28], where density of deposited energy equal to the total Si-O bonding energy of 3.8 eV in a unit volume of a-SiO_2 has been correlated with the structural changes. This critical density of deposited energy corresponds to 3.4×10^{23} eV/cm^3. In our case, for 90 MGy GR irradiation, density of deposited energy equals 1.25×10^{24} eV/cm^3, and for 1 MeV O irradiation with the fluence of 1×10^{14} ions/cm^2 we find deposited energy density equal to 9×10^{23} eV/cm^3 (we note damage cross section equals 1 nm^2, and applied ion fluence equals 1/nm^2). Therefore, in both cases similar changes to IR spectra occur at the same levels of deposited energy densities, and also similar values can be found for other SHI beams used. Therefore, SHI irradiations present very attractive option for simulating very high dose GR exposures to materials relevant for nuclear applications.

5. Conclusions

In this work, ion tracks in amorphous SiO_2 were measured using infrared spectroscopy. Obtained experimental results of ion track measurements show typical behaviour like thresholding and increase in size with stopping power. However, model parameters have to be tuned to unusual values to obtain satisfactory description, making this material suitable for comparison with other thermal spike models. Other ion track features like core-shell morphology and contribution of the nuclear stopping to final ion track size can be used for the same purpose. Here we show that analytical thermal spike model is able to reproduce ion track core features without invoking boiling criteria like in the case of inelastic thermal spike model. In addition, we show transfer of the nuclear stopping into the thermal spike is very efficient. Finally, it was shown how present approach could

be useful to simulate response of the a-SiO_2 to very high dose gamma rays exposures using ion irradiations preformed on much shorter timescales.

Acknowledgements

This work was supported by the Croatian Centre of Excellence for Advanced Materials and Sensors and by the Croatian Science Foundation (pr. no. 8127). This work was supported by the National Research Foundation of Korea (NRF) grant funded by the Korea government (MIST), NRF-2017M2A8A4017221. Declarations of interest: none.

Data availability statement

The raw data required to reproduce these findings are available on request. The processed data required to reproduce these findings are available in Tables 1-4.

References

[1] M. Toulemonde, C. Trautmann, E. Balanzat, K. Hjort, A. Weidinger, Track formation and fabrication of nanostructures with MeV-ion beams, Nucl. Instruments Methods Phys. Res. Sect. B Beam Interact. with Mater. Atoms. 216 (2004) 1–8. doi:10.1016/j.nimb.2003.11.013.

[2] M. Toulemonde, W. Assmann, C. Dufour, A. Meftah, F. Studer, C. Trautmann, Experimental Phenomena and Thermal Spike Model Description of Ion Tracks in Amorphisable Inorganic Insulators, Mat. Meddelelser Det K. Danske Vidensk. Selsk. 52 (2006) 263.

[3] N. Itoh, D.M. Duffy, S. Khakshouri, A.M. Stoneham, Making tracks: electronic excitation roles in forming swift heavy ion tracks, J. Phys. Condens. Matter. 21 (2009) 474205–14. doi:10.1088/0953-8984/21/47/474205.

[4] F. Aumayr, S. Facsko, A.S. El-Said, C. Trautmann, M. Schleberger, Single ion induced surface nanostructures: a comparison between slow highly charged and swift heavy ions, J. Phys. Condens. Matter. 23 (2011) 393001. doi:10.1088/0953-8984/23/39/393001.

[5] M. Toulemonde, W. Assmann, C. Dufour, A. Meftah, C. Trautmann, Nanometric transformation of the matter by short and intense electronic excitation: Experimental data

versus inelastic thermal spike model, Nucl. Instruments Methods Phys. Res. Sect. B Beam Interact. with Mater. Atoms. 277 (2012) 28–39. doi:10.1016/j.nimb.2011.12.045.

[6] F. Agulló-López, A. Climent-Font, Á. Muñoz-Martín, J. Olivares, A. Zucchiatti, Ion beam modification of dielectric materials in the electronic excitation regime: Cumulative and exciton models, Prog. Mater. Sci. 76 (2016) 1–58. doi:10.1016/j.pmatsci.2015.06.002.

[7] M. Karlušić, C. Ghica, R.F. Negrea, Z. Siketić, M. Jakšić, M. Schleberger, S. Fazinić, On the threshold for ion track formation in CaF2, New J. Phys. 19 (2017) 23023. doi:10.1088/1367-2630/aa5914.

[8] M. Karlušić, M. Jakšić, H. Lebius, B. Ban-d'Etat, R.A. Wilhelm, R. Heller, M. Schleberger, Swift heavy ion track formation in SrTiO 3 and TiO 2 under random, channeling and near-channeling conditions, J. Phys. D. Appl. Phys. 50 (2017) 205302. doi:10.1088/1361-6463/aa678c.

[9] E. Akcöltekin, T. Peters, R. Meyer, A. Duvenbeck, M. Klusmann, I. Monnet, H. Lebius, M. Schleberger, Creation of multiple nanodots by single ions, Nat. Nanotechnol. 2 (2007) 290–294. doi:10.1038/nnano.2007.109.

[10] E. Akcöltekin, S. Akcöltekin, O. Osmani, A. Duvenbeck, H. Lebius, M. Schleberger, Swift heavy ion irradiation of SrTiO3 under grazing incidence, New J. Phys. 10 (2008) 1–13. doi:10.1088/1367-2630/10/5/053007.

[11] S. Akcöltekin, E. Akcöltekin, T. Roll, H. Lebius, M. Schleberger, Patterning of insulating surfaces by electronic excitation, Nucl. Instruments Methods Phys. Res. Sect. B Beam Interact. with Mater. Atoms. 267 (2009) 1386–1389. doi:10.1016/j.nimb.2009.01.156.

[12] M. Karlušić, S. Akcöltekin, O. Osmani, I. Monnet, H. Lebius, M. Jakšić, M. Schleberger, Energy threshold for the creation of nanodots on SrTiO3 by swift heavy ions, New J. Phys. 12 (2010) 43009. doi:10.1088/1367-2630/12/4/043009.

[13] O. Ochedowski, O. Osmani, M. Schade, B.K. Bussmann, B. Ban-d'Etat, H. Lebius, M. Schleberger, Graphitic nanostripes in silicon carbide surfaces created by swift heavy ion irradiation., Nat. Commun. 5 (2014) 3913. doi:10.1038/ncomms4913.

[14] M. Karlušić, R. Kozubek, H. Lebius, B. Ban-d'Etat, R.A. Wilhelm, M. Buljan, Z. Siketić, F. Scholz, T. Meisch, M. Jakšić, S. Bernstorff, M. Schleberger, B. Šantić, Response of GaN to energetic ion irradiation: conditions for ion track formation, J. Phys. D. Appl. Phys. 48 (2015) 325304. doi:10.1088/0022-3727/48/32/325304.

[15] M. Karlušić, S. Bernstorff, Z. Siketić, B. Šantić, I. Bogdanović-Radović, M. Jakšić, M.

Schleberger, M. Buljan, Formation of swift heavy ion tracks on a rutile TiO<inf>2</inf> (001) surface, J. Appl. Crystallogr. 49 (2016) 1704–1712. doi:10.1107/S1600576716013704.

[16] F. Meinerzhagen, L. Breuer, H. Bukowska, M. Bender, D. Severin, M. Herder, H. Lebius, M. Schleberger, A. Wucher, A new setup for the investigation of swift heavy ion induced particle emission and surface modifications, Rev. Sci. Instrum. 87 (2016). doi:10.1063/1.4939899.

[17] P. Kluth, C.S. Schnohr, O.H. Pakarinen, F. Djurabekova, D.J. Sprouster, R. Giulian, M.C. Ridgway, A.P. Byrne, C. Trautmann, D.J. Cookson, K. Nordlund, M. Toulemonde, Fine structure in swift heavy ion tracks in amorphous SiO2, Phys. Rev. Lett. 101 (2008) 1–4. doi:10.1103/PhysRevLett.101.175503.

[18] M. Toulemonde, W.J. Weber, G. Li, V. Shutthanandan, P. Kluth, T. Yang, Y. Wang, Y. Zhang, Synergy of nuclear and electronic energy losses in ion-irradiation processes: The case of vitreous silicon dioxide, Phys. Rev. B - Condens. Matter Mater. Phys. 83 (2011) 1–9. doi:10.1103/PhysRevB.83.054106.

[19] M. Buljan, M. Karlušić, I. Bogdanović-Radović, M. Jakšić, K. Salamon, S. Bernstorff, N. Radić, Determination of ion track radii in amorphous matrices via formation of nano-clusters by ion-beam irradiation, Appl. Phys. Lett. 101 (2012) 103112. doi:10.1063/1.4751841.

[20] A. Benyagoub, M. Toulemonde, Ion tracks in amorphous silica, J. Mater. Res. 30 (2015) 1529–1543. doi:10.1557/jmr.2015.75.

[21] A. Ibarra, E.R. Hodgson, The ITER project: The role of insulators, Nucl. Instruments Methods Phys. Res. Sect. B Beam Interact. with Mater. Atoms. 218 (2004) 29–35. doi:10.1016/j.nimb.2003.12.048.

[22] S. Girard, J. Kuhnhenn, A. Gusarov, B. Brichard, M. Van Uffelen, Y. Ouerdane, A. Boukenter, C. Marcandella, Radiation effects on silica-based optical fibers: Recent advances and future challenges, IEEE Trans. Nucl. Sci. 60 (2013) 2015–2036. doi:10.1109/TNS.2012.2235464.

[23] O. Peña-Rodríguez, J. Manzano-Santamaría, A. Rivera, G. García, J. Olivares, F. Agulló-López, Kinetics of amorphization induced by swift heavy ions in α-quartz, J. Nucl. Mater. 430 (2012) 125–131. doi:10.1016/j.jnucmat.2012.07.001.

[24] G. Szenes, Ion-induced amorphization in ceramic materials, J. Nucl. Mater. 336 (2005) 81–89. doi:10.1016/j.jnucmat.2004.09.004.

[25] W.J. Weber, R.C. Ewing, C.R.A. Catlow, T.D. de la Rubia, L.W. Hobbs, C. Kinoshita, H. Matzke, A.T. Motta, M. Nastasi, E.K.H. Salje, E.R. Vance, S.J. Zinkle, Radiation effects in crystalline ceramics for the immobilization of high-level nuclear waste and plutonium, J. Mater. Res. 13

(1998) 1434–1484. doi:10.1557/JMR.1998.0205.

[26] M.C. Busch, A. Slaoui, P. Siffert, E. Dooryhee, M. Toulemonde, Structural and electrical damage induced by high-energy heavy ions in SiO2/Si structures, J. Appl. Phys. 71 (1992) 2596–2601. doi:10.1063/1.351078.

[27] M.C. Busch, A. Slaoui, E. Dooryhee, M. Toulemonde, Infrared spectrometry observations of SiO2 films irradiated by high energy heavy ions, Radiat. Eff. Def. Solids. 126 (1993) 229–232. doi:10.1080/10420159908229104.

[28] K. Awazu, S. Ishii, K. Shima, S. Roorda, J.L. Brebner, Structure of latent tracks created by swift heavy-ion bombardment of amorphous SiO2, Phys. Rev. B. 62 (2000) 3689–3698. doi:10.1103/PhysRevB.62.3689.

[29] T. Yang, Y. Gao, X. Huang, Y. Zhang, M. Toulemonde, J. Xue, S. Yan, Y. Wang, The transformation balance between two types of structural defects in silica glass in ion-irradiation processes, J. Non. Cryst. Solids. 357 (2011) 3245–3250. doi:10.1016/j.jnoncrysol.2011.05.017.

[30] P. Kluth, O.H. Pakarinen, F. Djurabekova, R. Giulian, M.C. Ridgway, A.P. Byrne, K. Nordlund, Nanoscale density fluctuations in swift heavy ion irradiated amorphous SiO2, J. Appl. Phys. 110 (2011). doi:10.1063/1.3671614.

[31] O. Peña-Rodríguez, J. Manzano-Santamaría, J. Olivares, A. Rivera, F. Agulló-López, Refractive index changes in amorphous SiO2 (silica) by swift ion irradiation, Nucl. Instruments Methods Phys. Res. Sect. B Beam Interact. with Mater. Atoms. 277 (2012) 126–130. doi:10.1016/j.nimb.2011.12.057.

[32] C. Rotaru, F. Pawlak, N. Khalfaoui, C. Dufour, J. Perrire, A. Laurent, J.P. Stoquert, H. Lebius, M. Toulemonde, Track formation in two amorphous insulators, vitreous silica and diamond like carbon: Experimental observations and description by the inelastic thermal spike model, Nucl. Instruments Methods Phys. Res. Sect. B Beam Interact. with Mater. Atoms. 272 (2012) 9–14. doi:10.1016/j.nimb.2011.01.022.

[33] J. Manzano-Santamaría, J. Olivares, A. Rivera, O. Peña-Rodríguez, F. Agulló-López, Kinetics of color center formation in silica irradiated with swift heavy ions: Thresholding and formation efficiency, Appl. Phys. Lett. 101 (2012). doi:10.1063/1.4757886.

[34] A. Benyagoub, S. Loffler, M. Rammensee, S. Klaumünzer, Ion-beam-induced plastic deformation in vitreous silica, Radiat. Eff. Def. Solids. 110 (1989) 217–219.

[35] A. Benyagoub, S. Klaumünzer, M. Toulemonde, Radiation-induced compaction and plastic

flow of vitreous silica, Nucl. Instruments Methods Phys. Res. Sect. B. 146 (1998) 449–454. doi:10.1016/S0168-583X(98)00478-9.

[36] T. Van Dillen, A. Polman, C.M. Van Kats, A. Van Blaaderen, Ion beam-induced anisotropic plastic deformation at 300 keV, Appl. Phys. Lett. 83 (2003) 4315–4317. doi:10.1063/1.1629793.

[37] E. Snoeks, A. Van Blaaderen, T. Van Dillen, C.M. Van Kats, M.L. Brongersma, A. Polman, Colloidal Ellipsoids with Continuously Variable Shape, Adv. Mater. 12 (2010) 1511–1514. doi:10.1002/1521-4095(200010)12:20<1511::AID-ADMA1511>3.3.CO;2-Y.

[38] G. Rizza, Y. Ramjauny, M. Hayoun, S. Perruchas, T. Gacoin, P. Kluth, M.C. Ridgway, Saturation of the ion-hammering effect for large non-hydrostatic capillarity stresses in colloidal silica nanoparticles., Nanotechnology. 22 (2011) 475302. doi:10.1088/0957-4484/22/47/475302.

[39] K. Awazu, X. Wang, M. Fijimaki, J. Tominaga, H. Aiba, Y. Ohki, T. Komatsubara, Elongation of gold nanoparticles in silica glass by irradiation with swift heavy ions, Phys. Rev. B - Condens. Matter Mater. Phys. 78 (2008) 1–8. doi:10.1103/PhysRevB.78.054102.

[40] M.C. Ridgway, R. Giulian, D.J. Sprouster, P. Kluth, L.L. Araujo, D.J. Llewellyn, A.P. Byrne, F. Kremer, P.F.P. Fichtner, G. Rizza, H. Amekura, M. Toulemonde, Role of thermodynamics in the shape transformation of embedded metal nanoparticles induced by swift heavy-ion irradiation, Phys. Rev. Lett. 106 (2011) 1–4. doi:10.1103/PhysRevLett.106.095505.

[41] E.A. Dawi, A.M. Vredenberg, G. Rizza, M. Toulemonde, Ion-induced elongation of gold nanoparticles in silica by irradiation with Ag and Cu swift heavy ions: track radius and energy loss threshold., Nanotechnology. 22 (2011) 215607. doi:10.1088/0957-4484/22/21/215607.

[42] C. Dufour, V. Khomenkov, G. Rizza, M. Toulemonde, Ion-matter interaction: the three-dimensional version of the thermal spike model. Application to nanoparticle irradiation with swift heavy ions, J. Phys. D. Appl. Phys. 45 (2012) 65302. doi:10.1088/0022-3727/45/6/065302.

[43] P.E. Coulon, J. Amici, M.C. Clochard, G. Rizza, S. Perruchas, V. Khomenkov, C. Dufour, I. Monnet, C. Grygiel, Ion-shaping of embedded gold hollow nanoshells into vertically aligned prolate morphologies, Nanotechnol. Mater. Devices Conf. NMDC 2016 - Conf. Proc. (2016) 1–12. doi:10.1109/NMDC.2016.7777112.

[44] O. Peña-Rodríguez, A. Prada, J. Olivares, A. Oliver, L. Rodríguez-Fernández, H.G. Silva-Pereyra, E. Bringa, J.M. Perlado, A. Rivera, Understanding the ion-induced elongation of silver nanoparticles embedded in silica, Sci. Rep. 7 (2017) 922. doi:10.1038/s41598-017-01145-0.

[45] M. Buljan, I. Bogdanović-Radović, M. Karlušić, U. V. Desnica, G. Dražić, N. Radić, P. Dubček, K. Salamon, S. Bernstorff, V. Holý, Formation of long-range ordered quantum dots arrays in amorphous matrix by ion beam irradiation, Appl. Phys. Lett. 95 (2009) 63104. doi:10.1063/1.3204007.

[46] M. Buljan, I. Bogdanović-Radović, M. Karlušić, U. V. Desnica, N. Radić, N. Skukan, G. Dražić, M. Ivanda, O. Gamulin, Z. Matej, V. Valeš, J. Grenzer, T.W. Cornelius, H.T. Metzger, V. Holý, Generation of an ordered Ge quantum dot array in an amorphous silica matrix by ion beam irradiation: Modeling and structural characterization, Phys. Rev. B. 81 (2010) 85321. doi:10.1103/PhysRevB.81.085321.

[47] M. Buljan, I. Bogdanović-Radović, M. Karlušić, U. V. Desnica, N. Radić, M. Jakšić, K. Salamon, G. Dražić, S. Bernstorff, V. Holý, Design of quantum dot lattices in amorphous matrices by ion beam irradiation, Phys. Rev. B - Condens. Matter Mater. Phys. 84 (2011) 155312. doi:10.1103/PhysRevB.84.155312.

[48] I. Bogdanović-Radović, M. Buljan, M. Karlušić, N. Skukan, I. Božičević, M. Jakšić, N. Radić, G. Dražić, S. Bernstorff, Conditions for formation of germanium quantum dots in amorphous matrices by MeV ions: Comparison with standard thermal annealing, Phys. Rev. B - Condens. Matter Mater. Phys. 86 (2012) 165316. doi:10.1103/PhysRevB.86.165316.

[49] M. Karlušić, M. Jakšić, M. Buljan, J. Sancho-Parramon, I. Bogdanović-Radović, N. Radić, S. Bernstorff, Materials modification using ions with energies below 1 MeV/u, Nucl. Instruments Methods Phys. Res. Sect. B Beam Interact. with Mater. Atoms. 317 (2013) 143–148. doi:10.1016/j.nimb.2013.02.053.

[50] J. Jensen, A. Razpet, M. Skupiński, G. Possnert, Ion track formation below 1 MeV/u in thin films of amorphous SiO 2, Nucl. Instruments Methods Phys. Res. Sect. B Beam Interact. with Mater. Atoms. 243 (2006) 119–126. doi:10.1016/j.nimb.2005.07.226.

[51] J. Jensen, A. Razpet, M. Skupiński, G. Possnert, Ion tracks in amorphous SiO2 irradiated with low and high energy heavy ions, Nucl. Instruments Methods Phys. Res. Sect. B Beam Interact. with Mater. Atoms. 245 (2006) 269–273. doi:10.1016/j.nimb.2005.11.072.

[52] A. Dallanora, T.L. Marcondes, G.G. Bermudez, P.F.P. Fichtner, C. Trautmann, M. Toulemonde, R.M. Papaléo, Nanoporous SiO2/Si thin layers produced by ion track etching: Dependence on the ion energy and criterion for etchability, J. Appl. Phys. 104 (2008) 1–8. doi:10.1063/1.2957052.

[53] A.M.J.F. Carvalho, M. Marinoni, A.D. Touboul, C. Guasch, H. Lebius, M. Ramonda, J. Bonnet, F.

Saigne, Discontinuous ion tracks on silicon oxide on silicon surfaces after grazing-angle heavy ion irradiation, Appl. Phys. Lett. 90 (2007) 7–9. doi:10.1063/1.2591255.

[54] A.M.J.F. Carvalho, A.D. Touboul, M. Marinoni, M. Ramonda, C. Guasch, F. Saigne, J. Bonnet, J. Gasiot, Oxide thickness dependence of swift heavy ion-induced surface tracks formation in silicon dioxide on silicon structures at grazing incidence, J. Appl. Phys. 102 (2007) 161–164. doi:10.1063/1.2826708.

[55] A.D. Touboul, A. Privat, R. Arinero, F. Wrobel, E. Lorfèvre, F. Saigné, Swift heavy ion-induced silicon dioxide nanostructuration: experimental observation of velocity effect, Eur. Phys. J. Appl. Phys. 60 (2012) 10402. doi:10.1051/epjap/2012120349.

[56] A. Meftah, M. Djebara, N. Khalfaoui, M. Toulemonde, Sputtering of vitreous SiO2 and Y3Fe5O12 in the electronic stopping power region: A thermal spike description, Nucl. Instruments Methods Phys. Res. Sect. B Beam Interact. with Mater. Atoms. 146 (1998) 431–436. doi:10.1016/S0168-583X(98)00496-0.

[57] N. Matsunami, M. Sataka, A. Iwase, Electronic sputtering of oxides by high energy heavy ion impact, Nucl. Instruments Methods Phys. Res. B. 193 (2002) 830–834. doi:10.1016/S0168-583X(02)00912-6.

[58] N. Matsunami, M. Sataka, A. Iwase, S. Okayasu, Electronic excitation induced sputtering of insulating and semiconducting oxides by high energy heavy ions, Nucl. Instruments Methods Phys. Res. Sect. B Beam Interact. with Mater. Atoms. 209 (2003) 288–293. doi:10.1016/S0168-583X(02)02050-5.

[59] W.M. Arnoldbik, P.A. ZeijImans Van Emmichoven, F.H.P.M. Habraken, Electronic sputtering of silicon suboxide films by swift heavy ions, Phys. Rev. Lett. 94 (2005) 1–4. doi:10.1103/PhysRevLett.94.245504.

[60] M. Toulemonde, W. Assmann, C. Trautmann, Electronic sputtering of vitreous SiO2: Experimental and modeling results, Nucl. Instruments Methods Phys. Res. Sect. B Beam Interact. with Mater. Atoms. 379 (2016) 2–8. doi:10.1016/j.nimb.2016.03.023.

[61] G. Szenes, The anisotropic growth in amorphous materials and the latent track formation induced by energetic ion bombardment, Nucl. Instruments Methods Phys. Res. Sect. B-Beam Interact. with Mater. Atoms. 107 (1996) 150–154. doi:Doi 10.1016/0168-583x(95)01021-1.

[62] H. Trinkaus, A. Ryazanov, Viscoelastic Model for the Plastic Flow of Amorphous Solids under Energetic Ion Bombardment, Phys. Rev. Lett. 74 (1995) 5072–5075. doi:10.1103/PhysRevLett.74.5072.

[63] M. Toulemonde, C. Dufour, E. Paumier, F. Pawlak, Does the latent track formation occurence in amorphous materials result from a transient thermal process?, MRS. 504 (1998) 99–110.

[64] S. Klaumünzer, Ion tracks in quartz and vitreous silica, Nucl. Instruments Methods Phys. Res. Sect. B Beam Interact. with Mater. Atoms. 225 (2004) 136–153. doi:10.1016/j.nimb.2004.05.014.

[65] S. Klaumünzer, Thermal-Spike Models for Ion Track Physics: A Critical Examination, Mat. Meddelelser Det K. Danske Vidensk. Selsk. 52 (2006) 293.

[66] S. Klaumünzer, Modification of nanostructures by high-energy ion beams, Nucl. Instruments Methods Phys. Res. Sect. B Beam Interact. with Mater. Atoms. 244 (2006) 1–7. doi:10.1016/j.nimb.2005.11.006.

[67] N. Itoh, A. Marshall Stoneham, Excitonic model of track registration of energetic heavy ions in insulators, Nucl. Instruments Methods Phys. Res. Sect. B Beam Interact. with Mater. Atoms. 146 (1998) 362–366. doi:10.1016/S0168-583X(98)00448-0.

[68] D.M. Duffy, S.L. Daraszewicz, J. Mulroue, Modelling the effects of electronic excitations in ionic-covalent materials, Nucl. Instruments Methods Phys. Res. Sect. B Beam Interact. with Mater. Atoms. 277 (2012) 21–27. doi:10.1016/j.nimb.2011.12.059.

[69] N. Medvedev, O. Osmani, B. Rethfeld, M. Schleberger, Track creation after swift heavy ion irradiation of insulators, Nucl. Instruments Methods Phys. Res. Sect. B Beam Interact. with Mater. Atoms. 268 (2010) 3160–3162. doi:10.1016/j.nimb.2010.05.078.

[70] N.A. Medvedev, A.E. Volkov, N.S. Shcheblanov, B. Rethfeld, Early stage of the electron kinetics in swift heavy ion tracks in dielectrics, Phys. Rev. B - Condens. Matter Mater. Phys. 82 (2010) 1–11. doi:10.1103/PhysRevB.82.125425.

[71] O. Osmani, N. Medvedev, M. Schleberger, B. Rethfeld, Energy dissipation in dielectrics after swift heavy-ion impact: A hybrid model, Phys. Rev. B - Condens. Matter Mater. Phys. 84 (2011) 1–9. doi:10.1103/PhysRevB.84.214105.

[72] N.A. Medvedev, R.A. Rymzhanov, A.E. Volkov, Time-resolved electron kinetics in swift heavy ion irradiated solids, J. Phys. D. Appl. Phys. 48 (2015) 355303. doi:10.1088/0022-3727/48/35/355303.

[73] J. Rzadkiewicz, O. Rosmej, A. Blazevic, V.P. Efremov, A. Gójska, D.H.H. Hoffmann, S. Korostiy, M. Polasik, K. Słabkowska, A.E. Volkov, Studies of the K?? X-ray spectra of low-density SiO2 aerogel induced by Ca projectiles for different penetration depths, High Energy Density Phys. 3 (2007) 233–236. doi:10.1016/j.hedp.2007.02.026.

[74] J. Rzadkiewicz, A. Gojska, O. Rosmej, M. Polasik, K. Słabkowska, Interpretation of the Si Kα x-ray spectra accompanying the stopping of swift Ca ions in low-density SiO2 aerogel, Phys. Rev. A - At. Mol. Opt. Phys. 82 (2010) 1–14. doi:10.1103/PhysRevA.82.012703.

[75] M. Karlušić, S. Fazinić, Z. Siketić, T. Tadić, D. Cosic, I. Božičević-Mihalić, I. Zamboni, M. Jakšić, M. Schleberger, Monitoring Ion Track Formation Using In Situ RBS/c, ToF-ERDA, and HR-PIXE, Materials (Basel). 10 (2017) 1041. doi:10.3390/ma10091041.

[76] N. Medvedev, A.E. Volkov, Femto-clock for the electron kinetics in swift-heavy ion tracks, J. Phys. D. Appl. Phys. (2017). doi:10.1016/j.jhazmat.2007.09.045.

[77] V. V Emeliyanov, A.S. Vatuev, R.G. Useinov, Impact of Heavy Ion Energy on Charge Yield in Silicon Dioxide, IEEE Trans. Nucl. Sci. (2018). doi:10.1109/TNS.2018.2813669.

[78] I. Bogdanović-Radović, M. Buljan, M. Karlušić, M. Jerčinović, G. Dražić, S. Bernstorff, R. Boettger, Modification of semiconductor or metal nanoparticle lattices in amorphous alumina by MeV heavy ions, New J. Phys. 18 (2016) 93032. doi:10.1088/1367-2630/18/9/093032.

[79] O. Tejayadi, Y.L. Sun, J. Klem, R. Fischer, M. V Klein, H. Morkoq, ORDER PARAMETERS IN a-Si SYSTEMS, Solid State Comm. 46 (1983) 251–254.

[80] J.F. Ziegler, M.D. Ziegler, J.P. Biersack, SRIM - The stopping and range of ions in matter (2010), Nucl. Instruments Methods Phys. Res. Sect. B Beam Interact. with Mater. Atoms. 268 (2010) 1818–1823. doi:10.1016/j.nimb.2010.02.091.

[81] G. Szenes, Comparison of two thermal spike models for ion-solid interaction, Nucl. Instruments Methods Phys. Res. Sect. B Beam Interact. with Mater. Atoms. 269 (2011) 174–179. doi:10.1016/j.nimb.2010.11.009.

[82] G. Szenes, An empirical equation between track radii and melting temperatures and its consequences for insulators irradiated by swift heavy ions, Nucl. Instruments Methods Phys. Res. Sect. B Beam Interact. with Mater. Atoms. 312 (2013) 118–121. doi:10.1016/j.nimb.2013.07.016.

[83] G. Szenes, General features of latent tracks in magnetic insulators irradiated by SHI, Phys. Rev. B. 51 (1995) 8026–8028.

[84] G. Szenes, Ion-induced temperature rise in various types of insulators, Radiat. Eff. Defects Solids. 170 (2015) 183–191. doi:10.1080/10420150.2014.996880.

[85] G. Szenes, Thermal spike analysis of ion-induced tracks in semiconductors, Nucl. Instruments Methods Phys. Res. Sect. B Beam Interact. with Mater. Atoms. 269 (2011) 2075–2079. doi:10.1016/j.nimb.2011.06.014.

[86] M. Toulemonde, W. Assmann, C. Trautmann, F. Grüner, Jetlike component in sputtering of LiF induced by swift heavy ions, Phys. Rev. Lett. 88 (2002) 576021–576024. doi:10.1103/PhysRevLett.88.057602.

[87] G. Szenes, Universal scaling for biomolecule desorption induced by swift heavy ions, Nucl. Instruments Methods Phys. Res. Sect. B Beam Interact. with Mater. Atoms. 233 (2005) 70–77. doi:10.1016/j.nimb.2005.03.088.

[88] G. Szenes, Thermal spike analysis of interface mixing induced by swift heavy ions, Appl. Phys. Lett. 81 (2002) 4622–4624. doi:10.1063/1.1528303.

[89] Z.G. Wang, C. Dufour, S. Euphrasie, M. Toulemonde, Electronic thermal spike effects in intermixing of bilayers induced by swift heavy ions, Nucl. Instruments Methods Phys. Res. Sect. B Beam Interact. with Mater. Atoms. 209 (2003) 194–199. doi:10.1016/S0168-583X(02)02028-1.

[90] S.K. Srivastava, D.K. Avasthi, W. Assmann, Z.G. Wang, H. Kucal, E. Jacquet, H.D. Carstanjen, M. Toulemonde, Test of the hypothesis of transient molten state diffusion for swift-heavy-ion induced mixing, Phys. Rev. B - Condens. Matter Mater. Phys. 71 (2005) 1–4. doi:10.1103/PhysRevB.71.193405.

[91] G. Szenes, Mixing of nuclear and electronic stopping powers in the formation of surface tracks on mica by fullerene impact, Nucl. Instruments Methods Phys. Res. Sect. B Beam Interact. with Mater. Atoms. 191 (2002) 27–31. doi:10.1016/S0168-583X(02)00508-6.

[92] A.S. El-Said, R. Heller, W. Meissl, R. Ritter, S. Facsko, C. Lemell, B. Solleder, I.C. Gebeshuber, G. Betz, M. Toulemonde, W. Möller, J. Burgdörfer, F. Aumayr, Creation of nanohillocks on CaF2 surfaces by single slow highly charged ions, Phys. Rev. Lett. 100 (2008) 2–5. doi:10.1103/PhysRevLett.100.237601.

[93] M. Karlušić, M. Jakšić, Thermal spike analysis of highly charged ion tracks, Nucl. Instruments Methods Phys. Res. Sect. B Beam Interact. with Mater. Atoms. 280 (2012) 103–110. doi:10.1016/j.nimb.2012.03.016.

[94] Y.Y. Wang, C. Grygiel, C. Dufour, J.R. Sun, Z.G. Wang, Y.T. Zhao, G.Q. Xiao, R. Cheng, X.M. Zhou, J.R. Ren, S.D. Liu, Y. Lei, Y.B. Sun, R. Ritter, E. Gruber, a Cassimi, I. Monnet, S. Bouffard, F. Aumayr, M. Toulemonde, Energy deposition by heavy ions: additivity of kinetic and potential energy contributions in hillock formation on CaF2., Sci. Rep. 4 (2014) 5742. doi:10.1038/srep05742.

[95] C. Dufour, V. Khomrenkov, Y.Y. Wang, Z.G. Wang, F. Aumayr, M. Toulemonde, An attempt to

apply the inelastic thermal spike model to surface modifications of CaF_2 induced by highly charged ions: comparison to swift heavy ions effects and extension to some others material, J. Phys. Condens. Matter. 29 (2017) 95001. doi:10.1088/1361-648X/aa547a.

[96] G. Szenes, Amorphous track formation in SiO2, Nucl. Instrum. Methods Phys. Res., Sect. B. 122 (1997) 530–533. doi:10.1016/S0168-583X(96)00660-X.

[97] G. Szenes, B. Pécz, Anomalous effect of ion velocity on track formation in GeS, Nucl. Instruments Methods Phys. Res. Sect. B Beam Interact. with Mater. Atoms. 389–390 (2016) 17–22. doi:10.1016/j.nimb.2016.11.008.

[98] R.A. Rymzhanov, N.A. Medvedev, A.E. Volkov, Effect of atomic structure on excitation of the electronic subsystem of a solid by a swift heavy ion, Nucl. Instruments Methods Phys. Res. Sect. B Beam Interact. with Mater. Atoms. 354 (2015) 292–296. doi:10.1016/j.nimb.2014.11.032.

[99] E.P. Donovan, F. Spaepen, D. Turnbull, J.M. Poate, D.C. Jacobson, Calorimetric studies of crystallization and relaxation of amorphous Si and Ge prepared by ion implantation, J. Appl. Phys. 57 (1985) 1795–1804. doi:10.1063/1.334406.

[100] A. Meftah, F. Brisard, J.M. Costantini, E. Dooryhee, M. Hage-Ali, M. Hervieu, J.P. Stoquert, F. Studer, M. Toulemonde, Track formation in SiO2 quartz and the thermal-spike mechanism, Phys. Rev. B - Condens. Matter Mater. Phys. B. 49 (1994) 12457–12463.

[101] C. Trautmann, J.M. Costantini, A. Meftah, K. Schwartz, J.P. Stoquert, M. Toulemonde, Swelling of SiO2 quartz induced by energetic heavy ions, Mat. Res. Soc. 504 (1998) 123. doi:10.1557/PROC-504-123.

[102] A. Rivera, J. Olivares, A. Prada, M.L. Crespillo, M.J. Caturla, E.M. Bringa, J.M. Perlado, O. Peña-Rodríguez, Permanent modifications in silica produced by ion-induced high electronic excitation: Experiments and atomistic simulations, Sci. Rep. 7 (2017) 1–14. doi:10.1038/s41598-017-11182-4.

[103] S.M.M. Ramos, C. Clerc, B. Canut, J. Chaumont, M. Toulemonde, H. Bernas, Damage kinetics in MeV gold ion - irradiated crystalline quartz, Nucl. Instruments Methods Phys. Res. Sect. B Beam Interact. with Mater. Atoms. 166 (2000) 31–34. doi:10.1016/S0168-583X(99)00735-1.

[104] M. Toulemonde, S.M.M. Ramos, H. Bernas, C. Clerc, B. Canut, J. Chaumont, C. Trautmann, MeV gold irradiation induced damage in α-quartz: Competition between nuclear and electronic stopping, Nucl. Instruments Methods Phys. Res. Sect. B Beam Interact. with Mater. Atoms. 178 (2001) 331–336. doi:10.1016/S0168-583X(00)00496-1.

[105] G. Szenes, Comment on Dense and nanometric electronic excitations induced by swift heavy ions in an ionic CaF2 crystal: Evidence for two thresholds of damage creation'', Phys. Rev. B - Condens. Matter Mater. Phys. 87 (2013) 2–4. doi:10.1103/PhysRevB.87.056101.

[106] P. Sigmund, P HYSICAL J OURNAL D Reciprocity in the electronic stopping of slow ions in matter, 54 (2008) 45–54. doi:10.1140/epjd/e2008-00011-9.